Image-Based Method for Retrospective Correction of Physiological Motion Effects in fMRI: RETROICOR

Gary H. Glover,[1*] Tie-Qiang Li,[1] and David Ress[2]

Respiration effects and cardiac pulsatility can induce signal modulations in functional MR image time series that increase noise and degrade the statistical significance of activation signals. A simple image-based correction method is described that does not have the limitations of *k*-space methods that preclude high spatial frequency correction. Low-order Fourier series are fit to the image data based on time of each image acquisition relative to the phase of the cardiac and respiratory cycles, monitored using a photoplethysmograph and pneumatic belt, respectively. The RETROICOR method is demonstrated using resting-state experiments on three subjects and compared with the *k*-space method. The method is found to perform well for both respiration- and cardiac-induced noise without imposing spatial filtering on the correction.   Magn Reson Med 44:162–167, 2000. © 2000 Wiley-Liss, Inc.
Key words: functional magnetic resonance imaging; physiological motion; retrospective motion correction

Functional Magnetic Resonance Imaging (fMRI) is based on changes in the signal resulting from blood oxygenation level dependence (BOLD) contrast (1,2) or blood flow changes (2). Pulsatility of blood flow in the brain and respiration-induced magnetic field changes or motion can cause appreciable modulation of the signal (3,4), which in turn causes undesired perturbations in the images that include intensity fluctuations and other artifacts. In many cases the added noise induced by these physiological processes can be comparable to the desired signal, which degrades the statistical significance of activation signals or otherwise compromises event-related analyses. Dagli et al. (5) have found that the effects of cardiac function tend to be rather localized in the brain as a result of vessel-dependent brain pulsatility. Respiration effects, which originate from thoracic modulation of the magnetic field in the head or from bulk motions of the head, are often more spatially global (3). However, we show here that respiration effects can also be localized.

Several methods have been developed for reducing such physiological noise in fMRI time series. Navigator methods correct *k*-space data using either an auxiliary echo (6) or the scan data themselves (7,8). Although navigator methods can be effective, they sample either a projection of the brain or the entire slice and therefore lack specificity in localizing the source of motion, which in turn can cause incomplete correction or can introduce fluctuations in quiescent parts of the brain. Biswal et al. (9) introduced the use of notch filters to remove components of the time-series spectrum at the cardiac and respiratory frequencies; this method fails, however, if the noise spectra alias into the region of the task spectrum. A retrospective correction method was introduced by Hu et al. (10) that fits a low-order Fourier series to the *k*-space time-series data based on the phase of the respiratory or cardiac cycle during each acquisition. This method was found to work particularly well for correcting respiratory effects and has been used for event-related experiments such as observation of the prompt response (11). However, only the data near the *k*-space origin have adequate signal-to-noise ratio (SNR) for the Fourier fit to be robust, and thus only low-order spatial corrections can be made; this, in turn, introduces correlation between pixels in the correction. If only a fraction of the *k*-space values needed to represent a localized region such as the area surrounding a vessel are corrected, the noise will be partially reduced only in the vessel region and spurious modulation will be introduced into other regions of the brain.

In this work we describe a retrospective correction technique similar to the method of Hu et al. (10), but operating in the image domain (dubbed RETROICOR). Image-based correction provides advantages in that spatial-frequency filtering is not imposed on the correction as with the *k*-space method, and therefore the correction functions equally well for both global and localized cardiac and respiratory noise. The concept was first introduced by Josephs et al. (12), who used SPM to generate maps of the physiological motion components. This approach was employed to diminish physiological noise in fMRI by modeling the electrocardiogram (ECG) and respiratory-phase waveforms as confounding signals (13). In many cases, however, correcting the data apart from performing a statistical analysis is desired, and thus the independent RETROICOR method was developed. The technique is demonstrated with resting-state brain data and compared with the *k*-space method of Hu et al. (10), called RETROKCOR for this work; their software implementation, which can perform corrections in *k*-space or image space, is available from http://www.cmrr.umn.edu/software/physioFix_userGuide.html.

MATERIALS AND METHODS

RETROICOR

The correction method assumes that the time series of intensities $y(t)$ in a pixel is corrupted by additive noise resulting from cardiac and respiratory functions. The cardiac and respiratory states are monitored during the scan using a photoplethysmograph and a pneumatic belt placed

around the subject's abdomen, respectively. It is assumed that the physiological processes are quasi-periodic so that cardiac and respiratory phases can be uniquely assigned for each image in the time series. Accordingly, the physiological noise component $y_\delta(t)$ can be expressed as a low-order Fourier series expanded in terms of these phases:

$$y_\delta(t) = \sum_{m=1}^{M} a_m^c \cos(m\varphi_c) + b_m^c \sin(m\varphi_c) + a_m^r \cos(m\varphi_r) + b_m^r \sin(m\varphi_r) \qquad [1]$$

where the superscript on coefficients a and b refers to cardiac or respiratory function, and $\phi_c(t)$ and $\phi_r(t)$ are the phases in the respective cardiac and respiratory cycles at time t. In this work $M = 2$ was used after preliminary studies showed that little was gained by including higher-order terms. With Eq. [1] evaluated, the data are corrected by subtracting $y_\delta(t)$ from $y(t)$.

Following Hu, the cardiac phase is defined as

$$\varphi_c(t) = 2\pi(t - t_1)/(t_2 - t_1) \qquad [2]$$

where t_1 is the time of the R-wave peak in the cardiac cycle just preceding t, and t_2 is the time for the subsequent R-wave peak. Thus, the cardiac phase is assumed to advance linearly from 0 to 2π during each R–R interval and is reset to 0 for the next cycle.

The respiratory phase must be assigned with some care. The NMR phase shifts that result in the head from magnetic field variations, as well as any bulk motion of the head from respiration, depend on the depth of the breathing cycle; thus, the respiratory phase cannot be calculated in the same way as the cardiac phase from just the times of peak inspiration, because the amplitude of the respiration should also be accounted for. Therefore, an alternative method is used that generates a histogram-equalized transfer function between respiratory amplitude and $\phi_r(t)$ (14). Let $R(t)$ be the amplitude of the respiratory signal from the pneumatic belt, which is normalized to the range (0, R_{max}). A histogram $H(b)$ is obtained as the number of occurrences H of respiratory values during the scan at bin values b, where 100 bins are chosen to span the range, and the bth bin is accordingly centered at $bR_{max}/100$. The running integral of $H(b)$ creates an equalized transfer function between R and respiratory phase, where end-expiration is assigned a phase of zero and peak inspiration has a phase of $\pm\pi$. While inhaling ($dR/dt > 0$), the phase spans 0 to π, whereas during expiration (when $dR/dt < 0$) the phase is negated. The transfer function that relates $\phi_r(t)$ to $R(t)$ is then given by

$$\varphi_r(t) = \pi \frac{\sum_{b=1}^{\text{rnd}[R(t)/R_{max}]} H(b)}{\sum_{b=1}^{100} H(b)} \text{sgn}(dR/dt) \qquad [3]$$

where rnd( ) denotes an integer-rounding operation. The derivative dR/dt is obtained by convolving $R(t)$ with a 39-point kernel, which is equivalent to performing a sliding quadratic least-squares fit to the data (15). This dura-

tion kernel includes almost 1 sec of data in the sliding fit, since $R(t)$ was sampled at 40 samples/sec.

The coefficients (a, b) in Eq. [1] are obtained for every pixel by a Fourier summation over all time points t_n:

$$a_m^x = \sum_{n=1}^{N} [y(t_n) - \bar{y}]\cos(m\varphi_x(t_n)) / \sum_{n=1}^{N} \cos^2(m\varphi_x(t_n))$$

$$b_m^x = \sum_{n=1}^{N} [y(t_n) - \bar{y}]\sin(m\varphi_x(t_n)) / \sum_{n=1}^{N} \sin^2(m\varphi_x(t_n)) \qquad [4]$$

where $x = (c, r)$, and $\bar{y}$ denotes the average of y over the time series. In the usual Fourier series, in which the cycle duration is fixed and an integral number of cycles is used, the denominators in Eq. [4] reduce to $N/2$, but in general that is not the case here. Caution should be exercised if task activation is time-locked to either respiration or cardiac function, because a valid activation signal will be subtracted by the correction. In this case, only resting-state baseline frames should be used and steps should be taken to make the task asynchronous with the physiological processes. This could occur, for example, in short-TR (repetition time), event-related experiments with subjects having highly regular breathing, or with task-related breathing changes.

Experiments

All experimental imaging data were obtained with a 3 T scanner equipped with high-performance gradients and receiver (GE Signa, rev 8.2.5, Milwaukee, WI). T_1-weighted FSE scans were acquired for anatomic reference (TR/spin-echo time (TE)/ETL = 68 msec/4000 msec/12). An automated high-order shimming method based on spiral acquisitions was employed to reduce B_0 heterogeneity. Resting-state "functional" acquisitions used a 2D spiral gradient-recalled echo sequence with TE 30 msec, field of view (FOV) 22 cm, and scan duration of 200 sec (8). The in-plane trajectory was a single-shot uniform-density spiral providing resolution of 2.3 mm (matrix 96 × 96). Either three or twelve 5 mm slices (depending on TR; see below) were acquired with axial scan plane. In Subject 3, oblique coronal planes nominally perpendicular to the calcarine fissure (often used when studying visual cortex) were also obtained. A homemade head coil was used for all scans and subjects were stabilized with foam padding packed tightly in the coil. Images were reconstructed into a 128 × 128 matrix with an off-line computer (Sun Microsystems, Mountain View, CA) using gridding and fast-Fourier transforms (FFTs). Linear shim corrections for each slice were applied during reconstruction using individual field maps obtained during the scan.

Two scans were obtained for each of three subjects at TRs of 250 msec (3 slices, 800 time frames each) and 1000 msec (12 slices, 200 frames). The shorter TR ensured that cardiac fluctuations in the images were resolved without temporal aliasing, whereas the longer TR provided more typical scan conditions in which cardiac pulsation could alias into spectral regions that overlap with those of the

Table 1
Percentage Signal in Cardiac and Respiratory Spectral Components, TR = 250 msec Scans*

Spectral component	Subject 1 (%)	Subject 2 (%)	Subject 3 (%)	Average ratio
Cardiac				
Uncorrected	0.54 (1.00)	1.64 (1.00)	1.19 (1.00)	
RETROKCOR	0.50 (0.93)	1.76 (1.07)	1.00 (0.84)	(0.95 ± 0.12)
RETROICOR	0.21 (0.39)	0.33 (0.20)	0.45 (0.38)	(0.32 ± 0.11)
Respiratory				
Uncorrected	1.65 (1.00)	0.70 (1.00)	0.32 (1.00)	
RETROKCOR	1.54 (0.93)	0.44 (0.63)	0.28 (0.88)	(0.81 ± 0.16)
RETROICOR	1.14 (0.69)	0.27 (0.38)	0.16 (0.50)	(0.52 ± 0.16)

*Numbers in parentheses represent ratio of corrected to uncorrected noise.

stimulus and respiration. The resting-state data were acquired with no intentional task, for which the subjects were instructed to keep their eyes closed.

Cardiac and respiratory functions were monitored using the scanner's built-in photoplethysmograph and respiratory belt. The photoplethysmograph sensor was placed on the subject's right index finger and the belt was positioned around the abdomen. The cardiac trigger and respiration data were recorded at a rate of 40 samples/sec using a multichannel data logger (MacLab, AD Instruments, Milford, MA) connected to the scanner's analog-gating outputs. The data logger was started by a trigger from the scanner to ensure time synchrony of the physiological and NMR data.

Data Analysis

RETROICOR

Following reconstruction, the images were corrected using RETROICOR with the cardiac and respiratory terms in Eq. [2] alone, as well as in combination. For each subject, one slice that maximized the cardiac and respiratory noise was chosen for further analysis. Time series for the corrected and uncorrected images were plotted using regions of interest (ROIs) in several brain areas. In addition, the time-series Fourier spectrum was calculated for every pixel and separate spatial distribution maps were obtained for the spectral components, which included the respiration and cardiac noise by summing the magnitude spectra over approximately ±0.05 Hz centered at the peaks. The peaks were identified from spectra of the physiological data and confirmed by comparing the uncorrected and RETROICOR-corrected spectra. These maps were overlaid on the anatomic images for orientation with the landmarks, but are presented here without the underlayment.

The noise components in the cardiac and respiration spectra were quantified for the short-TR data, for which these components were not aliased and could be unambiguously identified. The results were obtained using ROIs in the cardiac and respiratory noise maps, choosing regions in each map that maximized the noise. An additional ROI was chosen adjacent to the noise region as a measurement of the general background noise unrelated to cardiac function or respiration. The noise data corrected for the background were expressed as a percentage of the signal in the mean time-series image in the same ROIs.

RETROKCOR

The *k*-space method was implemented using corrections similar to the terms in Eq. [2] applied to the real and imaginary parts of the raw data before the normal gridding and FFT steps of reconstruction. Only the first 500 time points in the spiral data were employed, as the correction tended to become worse when more points were used. This subset contained about 75% of the energy in the *k*-space data. The reconstructed images were then submitted to the same analysis as for the RETROICOR method to obtain ROI time series, spectra, and spatial distribution maps of physiological noise components.

RESULTS

The technique is demonstrated here with detailed results for one subject (Subject 2 in Table 1). Results for the other subjects are summarized in tabular form.

Figure 1 shows the results for image time-series data in an ROI with TR 1000 msec, fitting separately to the cardiac (Fig. 1a) and respiratory (Fig. 1b) cycles. Note that both fits reveal underlying cycle-specific noise components. The time-series spectra are shown without (Fig. 1c) and with (Fig. 1d–f) corrections using the image-based method. Both cardiac and respiratory components were identified and substantially removed by the correction. In this case, the cardiac function is aliased and its spectrum overlaps partially with that from respiration, as is evident by comparing the uncorrected (Fig. 1c) and corrected (Fig. 1d) spectra. Figure 2 shows corresponding time series, without and with the image-based corrections.

Figure 3 presents similar results for the TR 250 msec scan. Both cardiac and respiratory functions are resolved at this TR, and the effect of applying the corrections is seen in the corresponding spectra. Maps of the noise energy at the cardiac and respiratory frequencies for the data corresponding to Fig. 3 are shown in Fig. 4 without correction, and with RETROICOR and RETROKCOR. The noise in the cardiac spectrum is localized near the frontal sinus, whereas the respiratory noise occurs in this slice in a medial region close to where the brain stem terminates more caudally and in other focal regions. The *k*-space method is less effective in reducing either form of noise than the image-based method.

The noise amplitudes in the cardiac and respiration spectra are presented in Table 1 for each of the subjects for
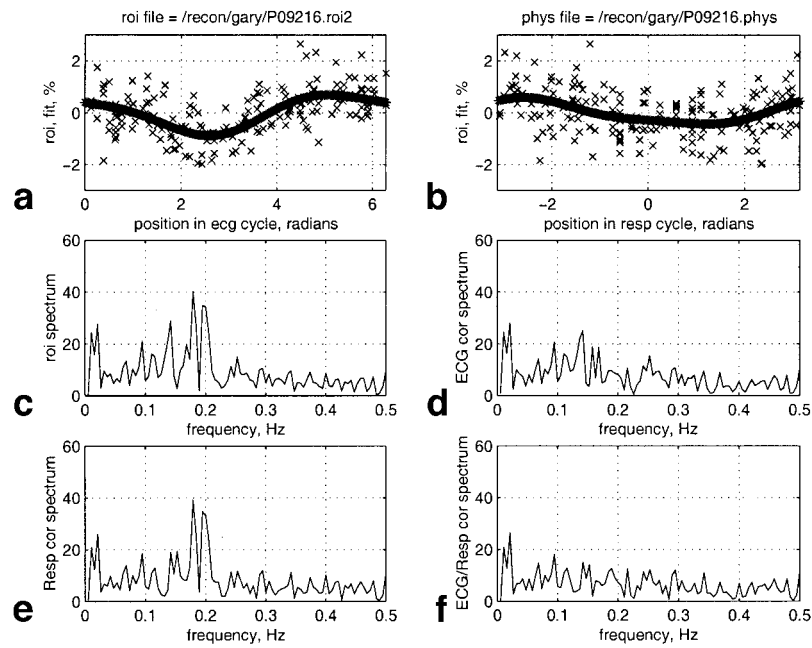
FIG. 1. RETROICOR method applied to ROI time-series data acquired at TR = 1000 msec. (**a**) Raw data (+) and y_δ cardiac fit (*) plotted vs. phase in cardiac cycle; (**b**) same data plotted vs. phase of respiratory cycle (+) and corresponding respiratory y_δ fit (*). Spectra of time series (**c**) without correction; (**d**) with cardiac correction alone; (**e**) with respiratory correction alone; (**f**) with both corrections. In this case the cardiac fluctuation spectrum (strong peak near 0.2 Hz) was aliased (heart rate 47 bpm) and partially overlapped with the respiratory spectrum (0.1–0.15 Hz).

both correction methods. As may be seen, the image-based method was effective in reducing the noise to a greater extent than the *k*-space method for all subjects, although there are insufficient data for statistical significance of the differences. However, the ROIs were deliberately chosen as worst-case; in most brain regions the residual corrected physiological noise is essentially unmeasurable over the background, as shown in Fig. 4.

DISCUSSION

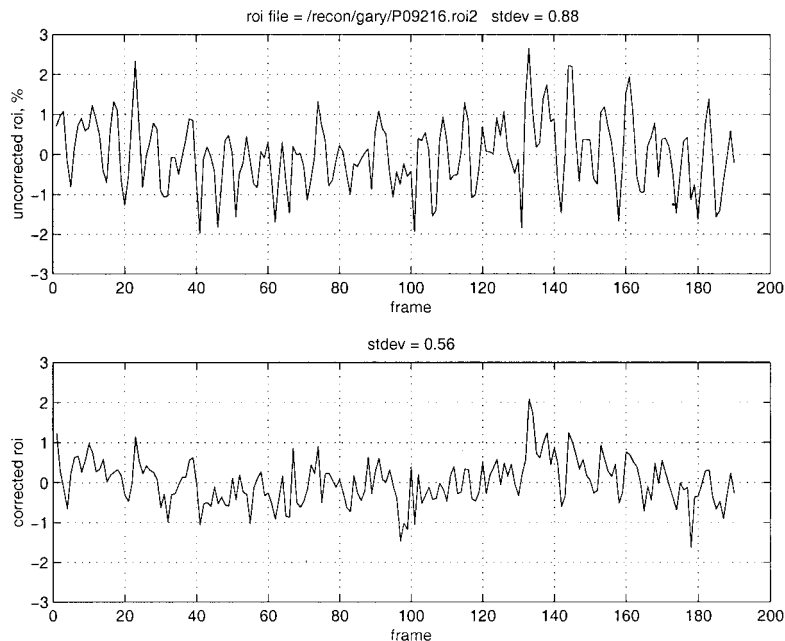The noise induced in fMRI time series by cardiac and respiratory functions can have different spatial character-

FIG. 2. Time series without (**top**) and with (**bottom**) RETROICOR correction corresponding to Fig. 1. Ordinate values are expressed as percentage of mean values.
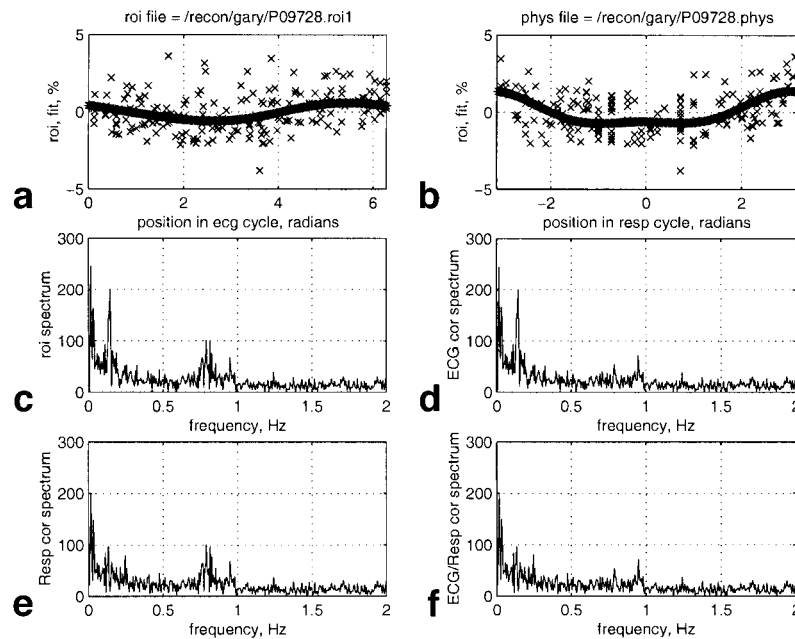
FIG. 3. RETROICOR method applied to ROI time-series data acquired at TR = 250 msec. (**a**) Raw data (+) and y_δ cardiac fit (*) plotted vs. phase in cardiac cycle; (**b**) same data plotted vs. phase of respiratory cycle (+) and corresponding respiratory y_δ fit (*). Only one-fourth of the 750 data points are plotted for clarity. Spectra of time series (**c**) without correction; (**d**) with cardiac correction alone; (**e**) with respiratory correction alone; (**f**) with both corrections. In this case the cardiac and respiratory spectra are resolved with peaks near 0.8 and 0.15 Hz, respectively.

istics. Cardiac pulsatility is often localized to edges of the brain such as near sulci or in tissue regions close to vessels such as the superior sagittal sinus. Some respiration-induced fluctuations result from longer-range effects such as small bulk movement of the head or magnetic field modulations from the changing state of the thoracic cavity. Image noise from this respiration component therefore tends to span the entire brain. In this case, noise associated with respiratory function occupies a smaller extent in k-space than circulatory-induced noise. However, as shown in Fig. 4, many regions of the brain have localized motion components tied to the respiratory cycle, perhaps

through brainstem motion. These effects are localized in a fashion similar to that of cardiac motion and thus occupy a similarly broad extent in k-space.

Retrospective correction methods that operate in k-space are limited to those spatial frequencies for which the SNR is adequate to ensure a good fit of the Fourier series to the data. This region includes only components close to the k-space origin, so that correlations in image space are introduced by the correction. This is not harmful for global respiration noise because of its low spatial frequency distribution, but can be detrimental for cardiac-induced noise or localized respiratory noise, since there
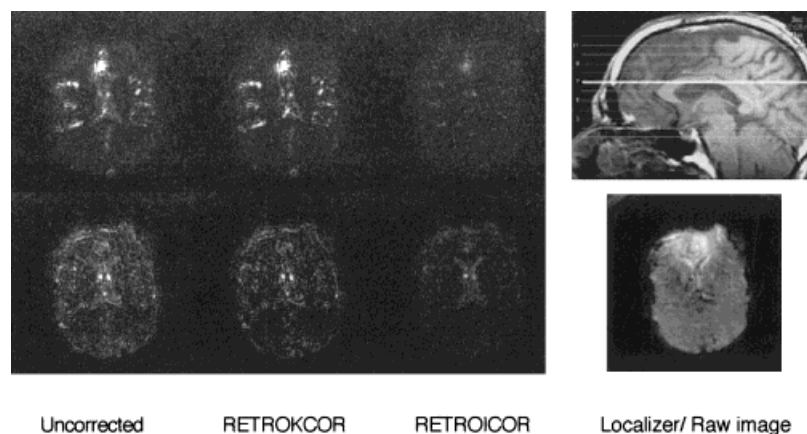

FIG. 4. Left: Maps of noise distributions for image data acquired at TR = 250 msec corresponding to Fig. 3, showing (**top**) cardiac components and (**bottom**) respiratory components. The three columns depict maps that are uncorrected, corrected with RETROKCOR, and corrected with RETROICOR, respectively. In this case the cardiac-related noise is highly localized, whereas the respiratory noise is more diffuse but shows some focal noise foci medially. Right: Localizer showing slice location, and T_2^*-weighted image.

may be insufficient *k*-space coverage to properly localize the correction. When this occurs, an average correction is applied that undercorrects the artifacts in regions of apparent high pulsatility and overcorrects other regions.

The RETROICOR method, in contrast with RETROKCOR, treats each pixel separately and therefore does not introduce artificial coupling of noise corrections across spatial regions. As a result, the RMS noise from cardiac and localized respiratory pulsatility was found to be reduced to a greater extent by the new method than by the *k*-space method. On the other hand, some degree of spatial correlation could be introduced into the correction, if desired, to improve the global respiratory correction by prefiltering the images to obtain a higher SNR before the Fourier coefficients are extracted. This smoothing step was not found necessary in this work.

An additional advantage of the method is that real-image data rather than complex raw data are corrected, which reduces the computational burden by half. Furthermore, because it is a postprocessing method operating on images, it may be easier to apply in practice than the *k*-space method because it is not necessary to invoke an off-line reconstruction after the corrections are made.

An assumption of the image-based correction is that each image is collected at a discrete time for which unique cardiac and respiratory phases can be assigned. This is a good assumption for single-shot imaging, but may not hold for multishot acquisitions, because the multiple-TR periods needed for all segments may span several cardiac or respiratory cycles. In this case the *k*-space method, in principle, may have an advantage because each segment can be separately corrected before combination during reconstruction. However, physiological image modulation is inherently reduced in multishot acquisitions, especially when navigation is employed (6,8), and we have found in practice that the method reduces the fluctuation noise as well with two-, three-, and four-shot acquisitions as with single-shot scans.

In summary, the retrospective image-based method appears to provide substantial reduction of additive noise components that arise from cardiac and respiratory functions. The sorting method is effective even when the noise is temporally aliased by undersampling, as confirmed by comparing the long- and short-TR scans. In addition, the new method can be applied to other quasi-periodic functions, as long as they can be monitored by an external transducer. One example is motion induced by subject responses such as verbal or finger movement. Caution should be used, however, that the physiological noise is asynchronous with task activation, to avoid reduction of the desired signals. Overall, RETROICOR may be useful in event-related fMRI experiments where added fluctuations in the time series are especially distracting, but may also find use in block-trial paradigms.

ACKNOWLEDGMENTS

REFERENCES

1. Ogawa S, Tank DW, Menon R, Ellermann JM, Kim SG, Merkle H, Ugurbil K. Intrinsic signal changes accompanying sensory stimulation: functional brain mapping with magnetic resonance imaging. Proc Natl Acad Sci USA 1992;89:5951–5955.
2. Kwong KK, Belliveau JW, Chesler DA, Goldberg IE, Weisskoff RM, Poncelet BP, Kennedy DN, Hoppel BE, Cohen MS, Turner R. Dynamic magnetic resonance imaging of human brain activity during primary sensory stimulation. Proc Natl Acad Sci USA 1992;89:5675–5679.
3. Noll DC, Schneider W. Theory, simulation and compensation of physiological motion artifacts in functional MRI. In: Proceedings of IEEE International Conference on Image Processing, Austin, Texas, 1994. p 40.
4. Glover GH, Lee AT. Motion artifacts in fMRI: comparison of 2DFT with PR and spiral scan methods. Magn Reson Med 1995;33:624–635.
5. Dagli MS, Ingeholm JE, Haxby JV. Localization of cardiac-induced signal change in fMRI. Neuroimage 1999;9:407–415.
6. Hu X, Kim SG. Reduction of signal fluctuation in functional MRI using navigator echoes. Magn Reson Med 1994;31:495–503.
7. Wowk B, McIntyre MC, Saunders JK. *k*-Space detection and correction of physiological artifacts in fMRI. Magn Reson Med 1997;38:1029–1034.
8. Glover GH, Lai S. Self-navigated spiral fMRI: interleaved versus single-shot. Magn Reson Med 1998;39:361–368.
9. Biswal B, DeYoe AE, Hyde JS. Reduction of physiological fluctuations in fMRI using digital filters. Magn Reson Med 1996;35:107–113.
10. Hu X, Le TH, Parrish T, Erhard P. Retrospective estimation and correction of physiological fluctuation in functional MRI. Magn Reson Med 1995;34:201–212.
11. Hu X, Le TH, Ugurbil K. Evaluation of the early response in fMRI in individual subjects using short stimulus duration. Magn Reson Med 1997;37:877–884.
12. Josephs O, Howseman AM, Friston K, Turner R. Physiological noise modelling for multi-slice EPI fMRI using SPM. In: Proceedings of the 5th Annual Meeting of ISMRM, Vancouver, Canada, 1997. p 1682.
13. Corfield DR, Murphy K, Josephs O, Fink GR, Frackowiak RS, Guz A, Adams L, Turner R. Cortical and subcortical control of tongue movement in humans: a functional neuroimaging study using fMRI. J Appl Physiol 1999;86:1468–1477.
14. Pelc N, Glover G. Method for reducing image artifacts due to periodic signal variations in NMR imaging. U.S. Patent 4 663 591,1987.
15. Savitzky A, Golay M. Smoothing and differentiation of data by simplified least squares procedures. Anal Chem 1964;36:1627–1639.

ERRATUM

In the article "Temperature Mapping Using the Water Proton Chemical Shift: Self-Referenced Method With Echo-Planar Spectroscopic Imaging," by K. Kuroda et al. (Vol. 43:220–225, 2000), the name of the last author was misspelled. The correct spelling should read: F.A. Jolesz.

We apologize for any inconvenience caused by this error.